Neuron
Report

Striatal Dopamine Release Is Triggered by Synchronized Activity in Cholinergic Interneurons

Sarah Threlfell,[1,2] Tatjana Lalic,[1] Nicola J. Platt,[1] Katie A. Jennings,[1] Karl Deisseroth,[3] and Stephanie J. Cragg[1,2,*]
[1]Department of Physiology, Anatomy, and Genetics, Sherrington Building, University of Oxford, Oxford OX1 3PT, UK
[2]Oxford Parkinson's Disease Centre, University of Oxford, Oxford OX1 3QX, UK
[3]Departments of Bioengineering, Psychiatry, and Behavioral Sciences, and Howard Hughes Medical Institute, Stanford University, Stanford, CA 94305, USA
*Correspondence: stephanie.cragg@dpag.ox.ac.uk
http://dx.doi.org/10.1016/j.neuron.2012.04.038

SUMMARY

Striatal dopamine plays key roles in our normal and pathological goal-directed actions. To understand dopamine function, much attention has focused on how midbrain dopamine neurons modulate their firing patterns. However, we identify a presynaptic mechanism that triggers dopamine release directly, bypassing activity in dopamine neurons. We paired electrophysiological recordings of striatal channelrhodopsin2-expressing cholinergic interneurons with simultaneous detection of dopamine release at carbon-fiber microelectrodes in striatal slices. We reveal that activation of cholinergic interneurons by light flashes that cause only single action potentials in neurons from a small population triggers dopamine release via activation of nicotinic receptors on dopamine axons. This event overrides ascending activity from dopamine neurons and, furthermore, is reproduced by activating ChR2-expressing thalamostriatal inputs, which synchronize cholinergic interneurons in vivo. These findings indicate that synchronized activity in cholinergic interneurons directly generates striatal dopamine signals whose functions will extend beyond those encoded by dopamine neuron activity.

INTRODUCTION

Striatal dopamine (DA) is critical to the regulation of motivation and movement. Disruptions to DA signaling underlie a variety of psychomotor disorders, including Parkinson's disease (PD) and addiction disorders. To understand striatal DA function, there has been intense study of when and how midbrain DA neurons change their firing rate, from tonic firing frequencies to intermittent bursts of action potentials at high frequencies. Current hypotheses posit that switches to phasic bursts of DA neuron activity and subsequent DA release encode motivational value and/or salience (Bromberg-Martin et al., 2010; Jin and Costa, 2010; Phillips et al., 2003; Redgrave et al., 2008; Schultz, 2010; Tsai et al., 2009) and regulate long-term changes in striatal synaptic plasticity (Owesson-White et al., 2008; Surmeier et al., 2009) that underpin action selection.

Action potentials in DA neurons have been assumed to be the principal trigger for DA transmission from striatal axons. How temporal or rate codes in DA neuron firing are relayed into DA release has been shown also to be modulated by presynaptic filters in DA axons that dynamically gate action potential-dependent DA release (Cragg, 2003; Montague et al., 2004). Although few in number, striatal cholinergic interneurons (ChIs) are thought to provide one such critical presynaptic mechanism through extensive striatal arborization (Contant et al., 1996) that supplies ACh to nicotinic receptors (nAChRs, β2-subunit containing) on DA axons (Jones et al., 2001). ChIs exhibit burst-and-pause changes that coincide with changes in DA neuron activity on presentation of salient stimuli (Ding et al., 2010; Morris et al., 2004). ChI pauses have been suggested to reduce DA release probability but promote the gain on DA signals when action potential frequency in DA neurons increases (Cragg, 2006; Rice and Cragg, 2004; Threlfell and Cragg, 2011; Zhang and Sulzer, 2004).

However, ChIs have been suggested to drive DA release from DA axons directly without requiring ascending activity in DA neurons (Ding et al., 2010). If physiological ACh release from ChIs can be demonstrated to evoke DA exocytosis, it would require us to radically reassess whether activity in DA neurons versus ChIs is the primary basis of DA function, to reappraise the outcome of coincident changes in activity in these neurons, and more generally to rethink the roles of inputs to neuronal axons versus soma. Here, we reveal such a mechanism, indicating that DA function can be independent of action potentials in DA soma; rather, activity in ChIs and their inputs that generate depolarization locally in DA axons have unexpectedly privileged importance in driving DA signals.

RESULTS AND DISCUSSION

To identify the effects of activation of striatal ChIs on DA transmission, we incorporated the light-activated ion channel channelrhodopsin2 (ChR2) into striatal ChIs of mice. ChR2 expression was restricted to ChIs by injecting an adeno-associated virus

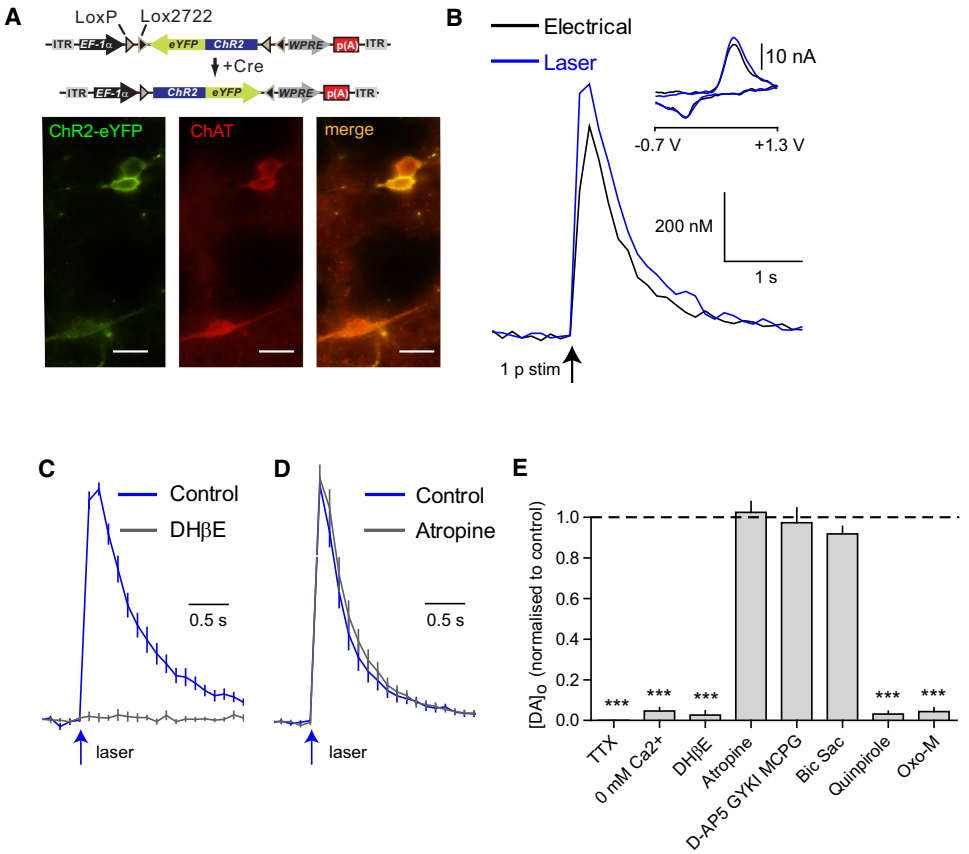

Figure 1. Activation of ChIs Drives Striatal Dopamine Release via nAChRs

(A) Schematic of Cre-dependent AAV ChR2(H134R)-eYFP; the gene is doubly flanked by two incompatible sets of loxP sites. Upon delivery into Cre-transgenics, ChR2-eYFP is inverted to enable transcription from the EF-1α promoter. Fluorescence shows ChR2-eYFP expression (green) in a population of ChIs (red). Scale bar represents 20 μm. (B) A local electrical or laser pulse (473 nm, 2 ms) in striatal slices evokes release of DA in CPu. Representative traces are shown. Inset: cyclic voltammograms identifying DA. (C and D) Mean DA release profiles (±SEM) in CPu after single laser pulse are prevented by antagonist of nAChRs (DHβE, 1 μM) (C) but not mAChRs (atropine, 2 μM) (D), n = 10–11. (E) Ionic and receptor dependence of ChI-driven DA release. TTX (1 μM); DHβE (1 μM); mAChR agonist oxotremorine (Oxo-M) (10 μM); DA D_2 receptor agonist quinpirole (1 μM); glutamate receptor antagonists: D-AP5 (50 μM), GYKI (10 μM), S-MCPG (200 μM); GABA receptor antagonists: bicuculline (bic, 10 μM), saclofen (sac, 50 μM). Data are means ± SEM.

(AAV) carrying a Cre-inducible ChR2 gene (fused inframe with the coding sequence for enhanced yellow fluorescent protein [eYFP]) into the striatum of transgenic mice expressing Cre-recombinase under the control of the promoter for choline acetyltransferase (ChAT) (Figure 1A) (also see Supplemental Information available online). In coronal slices that contain DA axons without DA soma, single blue laser flashes (1–2 ms; 473 nm) of ChR2-expressing terminals (15- to 60-μm-diameter spot) in dorsal or ventral striatum evoked the transient release and reuptake of DA, detected using fast-scan cyclic voltammetry (FCV) at carbon-fiber microelectrodes (see Supplemental Information) (n = 29 animals) (Figure 1B). Extracellular DA concentrations reached values similar to those evoked by local electrical stimuli (Figure 1B), indicating DA release from a population of axons. Light-evoked DA release was reproducible for several hours (sampling interval ~2.5 min) and required ACh activation of nAChRs. The β2-nAChR antagonist DHβE abolished DA release (Figure 1C; n = 10, $p < 0.001$) but not spiking in ChIs (Figure S1E, n = 3) indicating nAChRs postsynaptic to ChIs. ChI-driven DA release did not require muscarinic AChRs (mAChRs, Figure 1D, n = 11), glutamate receptors, or GABA receptors (Figure 1E, n = 9) but was modulated by mechanisms that normally gate ACh and/or DA exocytosis; it was abolished by Na_v^+-block by tetrodotoxin (TTX) (n = 10, $p < 0.001$), zero extracellular Ca^{2+} (n = 10, $p < 0.001$), D_2 receptor activation with quinpirole, (n = 8, $p < 0.001$), or mAChR activation with oxotremorine (n = 10, $p < 0.001$), which limits ACh release from ChIs (Threlfell et al., 2010) (Figure 1E). These observations indicate that endogenous ACh released from ChIs triggers DA release by activating axonal nAChRs, bypassing action potentials in DA soma.

To understand the neuronal events required for ChI-driven DA release, we paired recording of laser-evoked DA using FCV with whole-cell patch-clamp recording of ChR2-expressing, eYFP-tagged ChIs (see Supplemental Information) (Figure 2A). ChR2-expressing ChIs had normal resting membrane potential and TTX-sensitive action potentials (Figure S1; Table S1, n = 11). Laser-evoked DA release was seen after action potentials were evoked in local ChIs (latency 2.0 ± 0.5 ms, Figure 2B, n = 11).

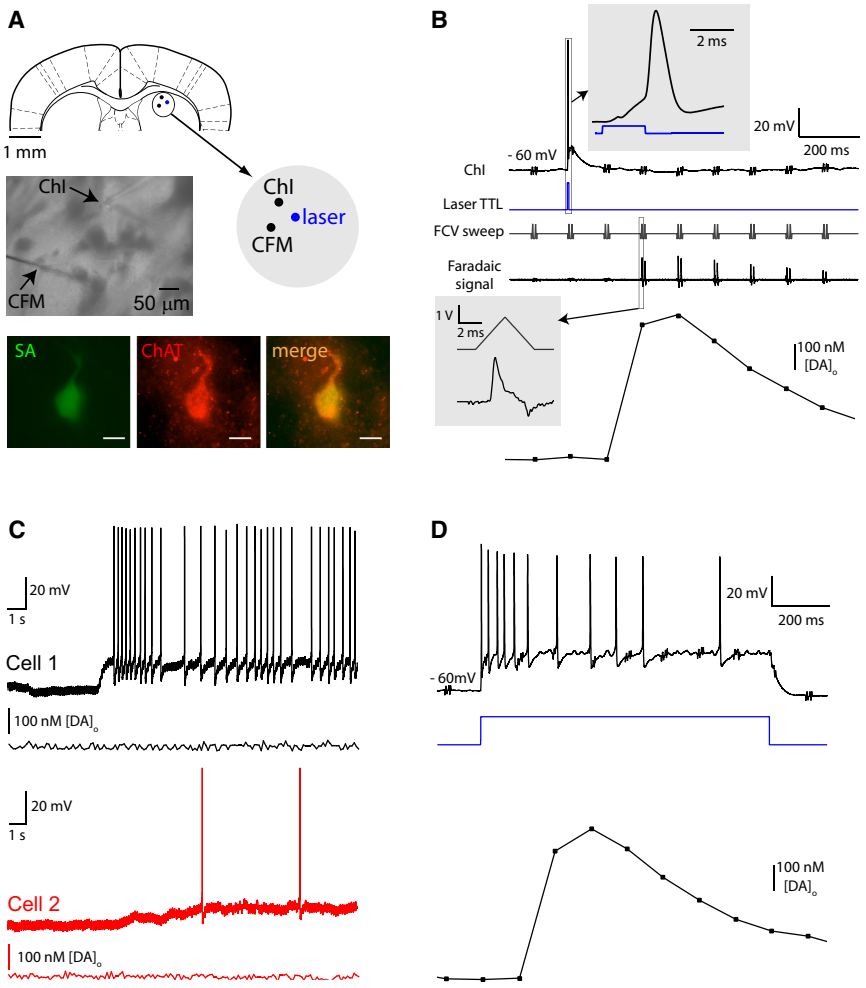

Figure 2. Synchronous Activity in Cholinergic Interneuron Population Evokes DA Release

(A) Schematic and IR-DIC image of recording configuration during combined recordings of ChI activity at patch electrode and DA at carbon-fiber microelectrode (CFM) in striatal slices from ChR2-eYFP-expressing ChAT-Cre mice. Bottom: eYFP-fluorescent ChIs were biocytin filled and identified using Alexa Fluor 488 streptavidin (SA, green) and coimmunoreactivity for ChAT (red). Scale bar represents 10 µm. (B) Representative example of simultaneous recordings of a single action potential in ChIs and DA release after a single laser pulse (2 ms, 10 mW/mm^2). Note FCV waveform (FCV sweep) generates 8 Hz artifact at patch electrode. Extracellular DA concentration versus time (bottom trace) is determined from DA oxidation current in background-subtracted voltammetric current (Faradaic signal), expanded in bottom inset. Top inset: short latency to spike after laser pulse (<2 ms; see Table S1). (C) Gradual increase in laser intensity (0–2 mW/mm^2) induces variable activity in different representative ChIs (cells 1 and 2) but no DA release. (D) Long laser pulse (1 s, 10 mW/mm^2) induces a burst of action potentials in ChI and DA release. See also Figure S1 and Table S1.

Short laser pulses that generated only one action potential in any recorded ChI were sufficient to evoke DA release (Figure 2B, n = 11); however, when we used current injection through the patch pipette (steps or ramps) to stimulate those same neurons individually to generate a single action potential, ongoing activity (1–2 Hz), or brief bursts, DA release was not evoked (Figure S1, n = 11) in ChAT-Cre or wild-type animals. One critical difference between current injection and a laser pulse is the number of neurons activated: the laser beam will synchronously activate a population of ChIs and/or their axons owing to the extensive overlapping arborization of ChI axons and dendrites (Contant et al., 1996). These data therefore suggest that ChI-driven DA release occurs during synchronization of activity in ChIs. The requirement for synchronization was confirmed by showing that laser stimuli that minimize synchrony in ChIs did not evoke DA release. To achieve this, we recruited activity gradually in a population of ChIs by slowly ramping laser intensity during continuous exposure until threshold for spiking was reached in a given recorded ChI. Using this protocol, outcome on activity in each ChI was variable (e.g., threshold intensity, see variation in spike frequency in Figure 2C, n = 6) and this protocol did not evoke DA release (Figure 2C, n = 6). Multiple spikes in a given ChI per se did not preclude DA release since longer duration laser pulses above threshold that evoked burst firing in ChIs were accompanied by DA release (Figure 2D, n = 11). These data show that synchronous recruitment of activity in a population of ChIs and/or axons evokes DA release.

We also noted that multiple action potentials in a given ChI induced by long laser pulses did not evoke more DA release than a single action potential (compare Figures 2D and 2B), suggesting that ChI-driven DA release does not convey frequency information from individual ChIs. This weak relationship between frequency and DA release is also seen with striatal electrical stimulation when DA axons and ChIs are simultaneously depolarized (Rice and Cragg, 2004; Zhang and Sulzer, 2004), but not with stimulation of medial forebrain bundle when DA axons are activated (Chergui et al., 1994). These observations suggest that ChI-driven DA release does not report frequency and moreover that it may limit how frequency information in ascending DA axons is transduced into DA release.

We therefore explored the relationships between frequency of activation and DA transmission during activation of ChIs only, DA axons only, or both in combination. Trains of four laser pulses at a range of frequencies in ChR2-expressing ChAT-Cre striatum reliably evoked four action potentials in ChIs at corresponding frequencies (Figure 3A), but the consequent DA release was invariant, reaching only DA levels seen with a single light pulse (and single action potentials) (Figures 3B and 3D, n = 8). This refractoriness (or depression) of rerelease after release by single

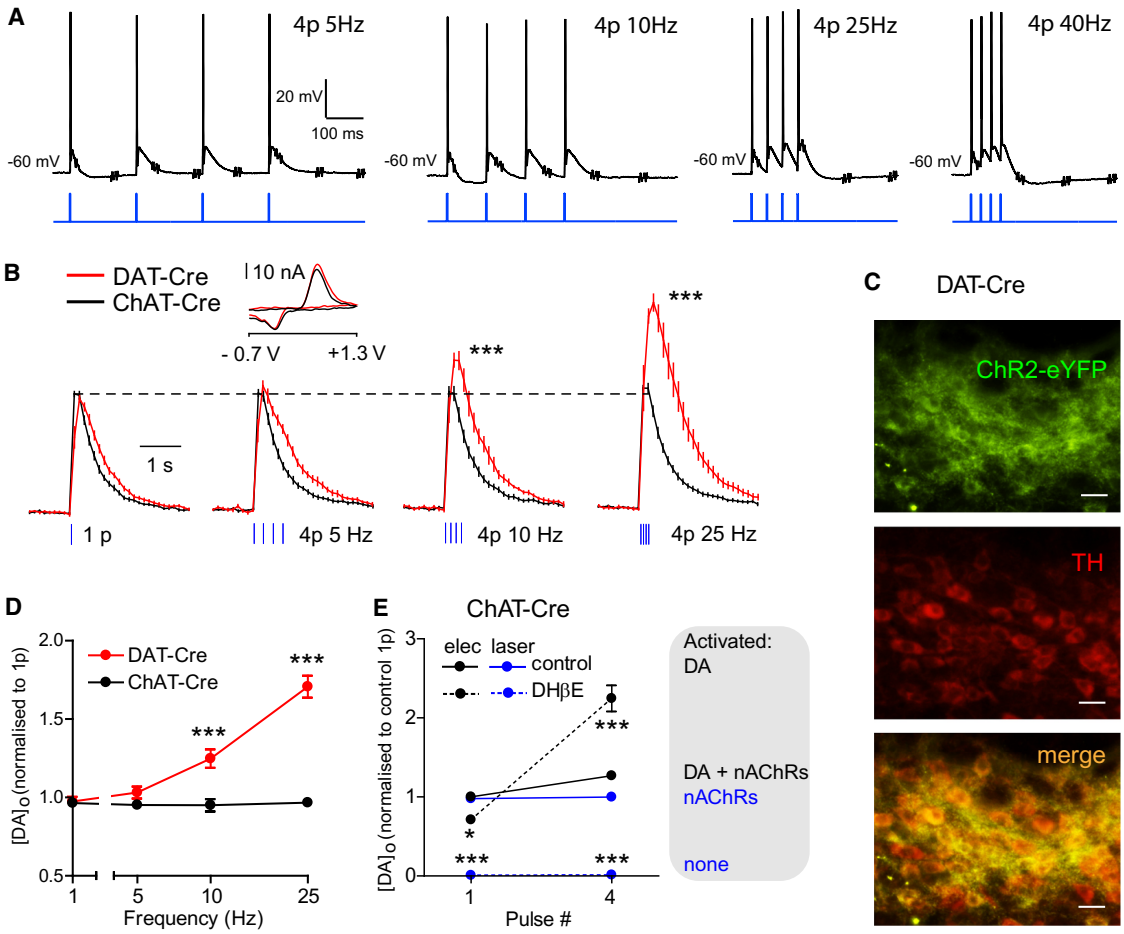

Figure 3. ChI-Driven DA Release Is Frequency Insensitive and Shunts DA Release Evoked by Ascending Activity

(A) Representative trace of ChR2-expressing ChIs following light pulses at various frequencies with corresponding action potentials. (B) Mean DA release profiles (±SEM) in CPu of ChR2-expressing ChAT-Cre (black) or DAT-Cre (red) mice after laser pulses (blue lines, 2 ms, 10 mW/mm^2) of different frequency, n = 6–9. Inset: cyclic voltammograms identifying DA. (C) Fluorescence shows ChR2-eYFP expression (green) in tyrosine hydroxylase-positive DA neurons (red) in SNc. Scale bar represents 20 μm. (D) Mean peak DA release in CPu is sensitive to frequency in ChR2-expressing DAT-Cre (red) ($p < 0.001$), but not ChR2-expressing ChAT-Cre (black), n = 6–9. (E) Effect on mean peak $[DA]_o$ of activating ChIs only (laser control), ChIs plus DA axons (elec control), or DA axons (elec DHβE) by single pulses versus four pulses at 100 Hz, obtained using light or local electrical stimuli in CPu from ChAT-Cre mice and using nAChR antagonist DHβE. Mean peak $[DA]_o$ varies with number of pulses after activating DA axons ($p < 0.001$) but not ChIs, with or without DA axon stimulation, n = 6. See also Figure S2. Data are means ± SEM.

synchronized spikes in ChIs was therefore not due to spike attenuation in ChIs (and was also not due to activation of mAChRs or D_2 receptors causing ACh terminal inhibition, data not shown). These data show that ChI-driven DA release is not a direct readout of the frequency of activity in a given ChI. By contrast, when DA release was evoked by laser activation of ChR2-expressing DA axons in striatum of DAT-Cre mice (Figure 3C; also see Supplemental Information; TTX sensitive, Ca^{2+} dependent, nAChR independent, Figure S2), DA release was sensitive to laser frequency (Figures 3B and 3D, n = 6–9, $p < 0.001$). As shown previously (Rice and Cragg, 2004; Zhang and Sulzer, 2004), when activation of DA axons occurs concurrently with nAChR activity, as occurs here using local electrical stimulation to evoke release of DA and ACh, the dominant outcome was frequency-insensitive DA release (in all genotypes) (Figure 3E, n = 6). Frequency sensitivity was restored with nAChR-antagonist DHβE (Figure 3E, $p < 0.001$). These data reveal further that the frequency insensitivity of ChI-driven DA release dominates over ascending activity in DA axons: ChI-driven DA release shunts the efficacy of concurrent activity in DA axons in evoking DA release. The mechanisms limiting the sensitivity of DA release to frequency are not known, but future studies should explore the role for dynamic changes in the plasticity of ACh or DA release or the nAChR effector mechanism, e.g., nAChR desensitization.

Our findings have several implications. First, the roles of excitability in axons versus soma in determining neurotransmitter release need to be reappraised. Activity in DA soma is not an exclusive trigger for axonal DA release; striatal ACh acting at nAChRs on DA axons bypasses midbrain DA neurons to trigger DA release directly. It has been suggested previously that nAChRs modulate the gain on action potential-elicited release (Rice and Cragg, 2004), but it has also been speculated from the effects of applied ACh or nicotine (Lambe et al., 2003; Léna et al., 1993; Wonnacott, 1997) that preterminal nAChRs might

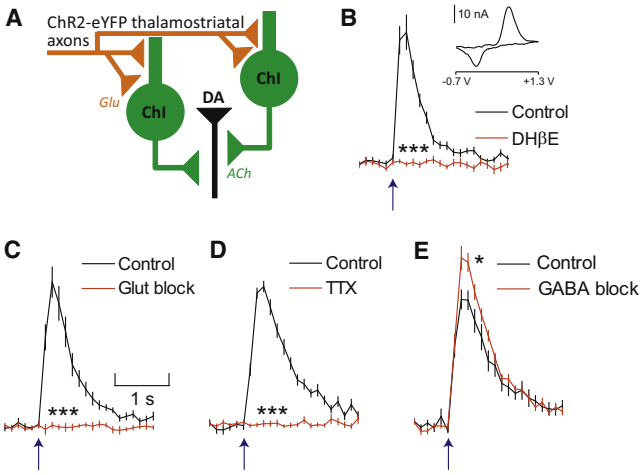

Figure 4. Activation of Thalamostriatal Axons Evokes ACh-Dependent DA Release

(A) Cartoon scheme of striatal connectivity between thalamostriatal afferents, ChIs, and DA axons. (B–E) Single laser/LED activation (473 nm, 2 ms) of ChR2-expressed thalamostriatal axons in striatal slices evokes release of DA in CPu that was prevented by inhibition of nAChRs (DHβE, 1 μM) (B), NMDA and AMPA glutamate receptors (D-AP5, 50μM; GYKI 52466, 10 μM) (C), as well as Na^+_v-channels with TTX (1 μM) (D), but not by inhibition of $GABA_A$ and $GABA_B$ receptors (bicuculine, 10 μM; saclofen 50 μM) (E). Mean ± SEM, n = 5. Inset in (B): cyclic voltammogram identifying DA.

trigger ectopic action potentials in axons. Our data now show that endogenous ACh released by single action potentials synchronized among ChIs does trigger DA release, via a direct preterminal action. These data also add to an accumulating body of evidence (Ding et al., 2010; Witten et al., 2010) suggesting that the long-held dogma of striatal ACh and DA acting only in opposition is outmoded and oversimplistic.

Second, these data indicate that circuits that activate striatal ChIs will have privileged roles as triggers of DA signals. What are the likely triggers and corresponding functions? Our data show that this ChI-driven DA signal is not a readout of activity in individual ChIs. But mechanisms that increase activity in ChIs in vivo should enhance the likelihood of synchronous activity in a subpopulation and bring this mechanism to threshold. Thus, ChI-driven DA release will reflect ChI population activity as a coincidence detector. Inputs that drive excitability and/or synchrony in ChIs could in turn be powerful triggers of DA signals. In vivo, ChI activity is strongly driven and synchronized across a network by thalamostriatal inputs, e.g., from intralaminar nuclei, that provide a rich innervation of networks of ChIs (as well as MSNs) (Ding et al., 2010; Goldberg and Reynolds, 2011; Morris et al., 2004; Raz et al., 1996; Smith et al., 2004) and that show stereotyped burst activity on presentation of salient stimuli (Aosaki et al., 1994; Matsumoto et al., 2001). We directly tested the intriguing possibility that activation of intralaminar thalamic glutamate inputs to striatum might also drive DA release via a striatal nAChR-dependent mechanism. Indeed, laser activation of ChR2-eYFP-expressing thalamostriatal axons arising from intralaminar thalamus in CaMKII-Cre mice evoked DA release in coronal striatal slices, and this was prevented by nAChR inhibition and, necessarily, glutamate receptor antagonists but not GABA receptor antagonists (Figure 4; n = 4 animals, TTX-sensitive, Ca^{2+}-dependent). ACh-dependent DA signals can therefore be driven by the thalamic inputs that synchronize activity in ChIs in vivo. It is interesting in this regard that the relatively "digital" nature of the stereotyped burst activity in the thalamostriatal network that is associated with salient event detection parallels the lack of simple frequency dependence in the ChI activation of DA release seen here. In any event, these data suggest that DA may be important for conveying salience- or attention-related signals mediated not through changes in DA neuron firing but through activation of DA axons by ChIs and their inputs.

Third, we would expect that a ChI-driven DA signal will have key outcomes for DA functions that are encoded by dynamic patterns of activity in DA neurons themselves. The outcome will depend entirely on the timing of activity in DA neurons relative to ChIs. Pauses in ChIs have been suggested previously to remove a low-pass filter on DA release during concurrent changes in DA neuron activity (Cragg, 2006). Prior ChI-driven DA release could shunt (limit) the impact of subsequent changes in DA neuron activity, while alternatively, postpause "rebound" facilitation in ChI activity (Aosaki et al., 1995; Apicella, 2007; Morris et al., 2004), which probably corresponds to increased synchrony in the population, could critically supplement preceding DA signals and promote, for example, the selection of a behavior. In addition, discrete functions for DA could be driven by synchronous activity in ChIs despite an absence of accompanying phasic changes in DA neuron activity, which otherwise would be taken as evidence for functions not requiring phasic DA. Furthermore, what might be the outcome for nicotine action? By desensitizing nAChRs on DA axons, nicotine would be expected to prevent ChI-driven DA release (pilot observations suggest this to be the case, data not shown) and thereby devolve the control of DA release to activity in DA neurons without modulation by ChIs. In this case, DA release might be a more direct reporter of activity in DA neurons than with nAChRs active (Rice and Cragg, 2004). Hypo- or hypercholinergic states implicated in basal ganglia disorders including PD, Huntington's, Tourette's, and dystonia and in the actions of addictive drugs could correspondingly result in the behavioral dysfunctions that underlie each of these disorders.

In summary, we show that endogenous striatal ACh release by synchronized activity in ChIs is sufficient to evoke DA release and thereby uncouple DA release from its relationship to activity in DA neurons. This mechanism may clamp or reinforce DA release triggered by ascending activity from DA axons depending on timing and could endow ChIs and DA with key functions that go beyond those identified from DA neuron recordings in the processes underpinning action selection.

EXPERIMENTAL PROCEDURES

Virus Injections and Slice Preparation

To generate expression of ChR2 in ChIs, DA neurons, or thalamostriatal glutamate inputs, we used a Cre-loxP approach by injecting a Cre-inducible recombinant AAV vector containing ChR2 (pAAV-double floxed-hChR2(H134R)-EYFP-WPRE-pA) in mice expressing Cre-recombinase in choline acetyltransferase (ChAT)-, dopamine transporter (DAT)-, or

Ca^{2+}-calmodulin-dependent kinase II (CaMKII)-positive neurons, respectively. Transgenic mice were bred from homozygotes for ChAT-internal ribosome entry site (IRES)-Cre, DAT-IRES-Cre, or CaMKII-Cre obtained from Jackson Laboratories (B6.129S6-*Chat*$^{tm1(cre)Lowl}$/J, stock 006410; B6.SJL-*Slc6a3*$^{tm1.1(cre)Bkmn}$ /J, stock 006660; B6.Cg-Tg(Camk2a-cre)T29-1Stl/J, stock 005359). The experimental data presented in this paper are from ChAT-Cre homozygote (and heterozygote, data not shown), DAT-Cre heterozygote, or CaMKII-Cre homozygote mice aged 2–8 months. Mice were anaesthetised with isoflurane, placed in a stereotaxic frame, and a craniotomy was performed. Bilateral intracerebral injections of a Cre-inducible recombinant AAV (1 μl per site for ChAT-Cre and DAT-Cre mice, 300 nl per site for CaMKII-Cre mice) were made with a 2.5 μl, 33 gauge Hamilton syringe using a microinjector at 0.2 μl/min. In ChAT-Cre mice, injections were made in dorsal CPu (AP +1.0 mm, ML ±1.8 mm, DV −2.2 mm) and in contralateral NAc core (AP +1.0 mm, ML ±1.0 mm, DV −4.0 mm). In DAT-Cre mice, injections were made in SNc (AP −3.5 mm, ML ±1.2 mm, DV −4.0 mm) and in contralateral VTA (AP −3.1 mm, ML ±0.5 mm, DV −4.4 mm). In CaMKII-Cre mice, injections were made in the intralaminar nucleus of the thalamus (AP −2.3, ML ±0.5, DV −3.4 mm). Wild-type C57BL/6 mice used in some experiments were aged postnatal days (P) 14–P22.

On days 12–76 postinjection, mice were decapitated after cervical dislocation or halothane anesthesia (for combined patch-clamp/FCV recordings). Coronal slices, 300 μm thick, containing CPu and NAc were prepared as described previously in ice-cold HEPES-buffered artificial cerebrospinal fluid (aCSF) or high-sucrose aCSF (for electrophysiology, see below) saturated with 95% O_2/5% CO_2. Slices were then maintained in a bicarbonate-buffered aCSF at room temperature prior to recording. During recordings, neurons were visualized on an upright microscope (Olympus BX51WI) equipped with IR-DIC, fluorescence optics for visualizing eYFP, and a charge-coupled device (CCD) camera.

Fast-Scan Cyclic Voltammetry

Slices were superfused with a bicarbonate-buffered aCSF maintained at 30°C–32°C as described previously (Rice and Cragg, 2004; Threlfell et al., 2010). Extracellular DA concentration ($[DA]_o$) was monitored using fast-scan cyclic voltammetry (FCV) with 7-μm-diameter carbon fiber microelectrodes (CFMs; tip length 50–100 μm) and a Millar voltammeter (Julian Millar, Barts and the London School of Medicine and Dentistry) as described previously (Threlfell et al., 2010). In brief, the scanning voltage was a triangular waveform (−0.7V to +1.3V range versus Ag/AgCl) at a scan rate of 800V/s and sampling frequency of 8 Hz. Electrodes were calibrated in 1–2 μM DA in each experimental media. For further details, see Supplemental Experimental Procedures.

Electrophysiology

For whole-cell patch-clamp studies (in isolation or in combination with FCV), 300 μm coronal slices containing CPu and NAc were prepared in ice-cold high-sucrose aCSF containing 85 mM NaCl, 25 mM $NaHCO_3$, 2.5 mM KCl, 1.25 mM NaH_2PO_4, 0.5 mM $CaCl_2$, 7 mM $MgCl_2$, 10 mM glucose, and 75 mM sucrose after decapitation under halothane anesthesia. Slices were then transferred to oxygenated aCSF (95% O_2/5% CO_2) containing 130 mM NaCl, 25 mM $NaHCO_3$, 2.5 mM KCl, 1.25 mM NaH_2PO_4, 2 mM $CaCl_2$, 2 mM $MgCl_2$, and 10 mM glucose at 35°C for 30–45 min and then maintained at room temperature until recording. During recordings, slices were superfused with aCSF saturated with 95% O_2/5% CO_2 at 32°C. Whole-cell patch-clamp electrodes (4–7 MΩ) were filled with an intracellular solution containing 120 mM K-gluconate, 10 mM KCl, 10 mM HEPES, 4 mM MgATP, 0.3 mM NaGTP, 10 mM Na-phosphocreatine, and 0.5% biocytin. ChIs in the striatum were identified by their distinctive morphological features (Figure S1A) (large somas and thick primary dendrites) and their characteristic electrophysiological properties, prominent Ih, AHP, and broad action potential (Figures S1B–S1D, Table S1). Intracellular recordings were obtained using a Multiclamp 700B amplifier and digitized at 10–20 kHz using Digidata 1440A acquisition board. While performing current-clamp recordings, a small amount of holding current (typically <−25 pA) was injected when necessary to keep the cell close to its initial resting membrane potential (−60mV). Biocytin was included in the intracellular solution to allow post hoc visualization and confirmation of cell identity. All data were analyzed offline with Clampfit (pClamp 10), Neuromatic (http://neuromatic.thinkrandom.com), and custom-written software running within IgorPro environment.

Light and Electrical Stimulation

ChR2-expressing fibers were activated using a 473 nm diode laser (DL-473, Rapp Optoelectronic) coupled to the microscope with a fiber optic cable (200 μm multimode, NA 0.22), which illuminated a 15- to 60-μm-diameter spot (40×/10× water-immersion objectives) or, in CaMKII experiments, an LED system (OptoLED, CAIRN) (see Supplemental Experimental Procedures). TTL-driven laser pulses (1–2 ms duration, 2–40 mW/mm^2 at specimen) or electrical pulses (0.6–0.7 mA, 200 μs) were delivered at a variety of frequencies designed to mimic physiological firing frequencies. Light power at microscope objective exit was 2–40 mW/mm^2 (see Figure S2). Electrical stimulation was delivered evoked by a local bipolar concentric electrode (25 μm diameter, Pt/Ir; FHC). Both light and electrical stimuli were delivered locally; the laser spot was out of field of view of the CFM (~200–300 μm from CFM) and stimulating electrode was placed ~150 μm from the CFM. Mean peak light-evoked $[DA]_o$ in dorsal CPu from ChAT-Cre (1.4 ± 0.2 μM) or DAT-Cre (1.0 ± 0.1 μM) was not significantly different ($n = 24$, $p > 0.05$). Data presented here is from dorsal CPu; however, we made similar observations in NAc (data not shown).

Statistical Analysis

Data were acquired and analyzed using Axoscope 10.2 (Molecular Devices) and locally written programs. Data are represented as means ± SEM, and "n" refers to the number of observations. The number of animals in each data set is ≥3. Data are expressed as extracellular concentration of dopamine ($[DA]_o$), or as $[DA]_o$ normalized to a single pulse in control. Comparisons for statistical significance were assessed by one- or two-way ANOVA and post hoc multiple-comparison t tests or unpaired t tests using GraphPad Prism. Levels of DA indicated either after current-induced activity in ChIs (Figures S1F–S1H) or while gradually increasing laser power from 0 mW/mm^2 until spike threshold is reached in single ChIs (Figure 2C) were indistinguishable from noise.

Drugs

D(-)-2-Amino-5-phosphonovaleric acid (D-AP5), 4-(8-methyl-9*H*-1,3-dioxolo[4,5-*h*][2,3]benzodiazepin-5-yl)-benzenamine hydrochloride (GYKI 52466 hydrochloride), (*S*)-α-methyl-4-carboxyphenylglycine [(*S*)-MCPG], oxotremorine-M (Oxo-M), bicuculline methiodide, and saclofen were purchased from Tocris Bioscience or Ascent Scientific. Atropine, dihydro-β-erythroidine (DHβE), and all other reagents were purchased from Sigma-Aldrich. Drugs were dissolved in distilled water, aqueous alkali [(*S*)-MCPG], or aqueous acid (GYKI 52466 hydrochloride) to make stock aliquots at 1,000–10,000× final concentrations and stored at −20°C until required. Stock aliquots were diluted with oxygenated aCSF to final concentration immediately before use.

Immunocytochemistry

To determine the specificity of ChR2 expression in ChAT-Cre or DAT-Cre mice, we fixed acute striatal (ChAT) or midbrain slices (DAT) containing ChR2-eYFP positive neurons postrecording and processed them for ChAT and/or TH and/or biocytin immunoreactivity. Immunoreactivity was visualized using fluorescent secondary antibodies (see Supplemental Experimental Procedures).

SUPPLEMENTAL INFORMATION

Supplemental Information includes two figures, one table, and Supplemental Experimental Procedures and can be found with this article online at http://dx.doi.org/10.1016/j.neuron.2012.04.038.

ACKNOWLEDGMENTS

We thank Neil Blackledge, Rob Klose, Diogo Pimentel, Ole Paulsen, Dennis Kaetzel, Gero Miesenbock, P. Wendy Tynan, and Oxford Biomedical Services for their invaluable input. This work was supported by a Parkinson's UK

Monument Trust Discovery Award and Parkinson's UK Grants G-0808 and G-0803, the Royal Society, and the MRC.

Accepted: April 25, 2012
Published: July 11, 2012

REFERENCES

Aosaki, T., Graybiel, A.M., and Kimura, M. (1994). Effect of the nigrostriatal dopamine system on acquired neural responses in the striatum of behaving monkeys. Science *265*, 412–415.

Aosaki, T., Kimura, M., and Graybiel, A.M. (1995). Temporal and spatial characteristics of tonically active neurons of the primate's striatum. J. Neurophysiol. *73*, 1234–1252.

Apicella, P. (2007). Leading tonically active neurons of the striatum from reward detection to context recognition. Trends Neurosci. *30*, 299–306.

Bromberg-Martin, E.S., Matsumoto, M., and Hikosaka, O. (2010). Dopamine in motivational control: rewarding, aversive, and alerting. Neuron *68*, 815–834.

Chergui, K., Suaud-Chagny, M.F., and Gonon, F. (1994). Nonlinear relationship between impulse flow, dopamine release and dopamine elimination in the rat brain in vivo. Neuroscience *62*, 641–645.

Contant, C., Umbriaco, D., Garcia, S., Watkins, K.C., and Descarries, L. (1996). Ultrastructural characterization of the acetylcholine innervation in adult rat neostriatum. Neuroscience *71*, 937–947.

Cragg, S.J. (2003). Variable dopamine release probability and short-term plasticity between functional domains of the primate striatum. J. Neurosci. *23*, 4378–4385.

Cragg, S.J. (2006). Meaningful silences: how dopamine listens to the ACh pause. Trends Neurosci. *29*, 125–131.

Ding, J.B., Guzman, J.N., Peterson, J.D., Goldberg, J.A., and Surmeier, D.J. (2010). Thalamic gating of corticostriatal signaling by cholinergic interneurons. Neuron *67*, 294–307.

Goldberg, J.A., and Reynolds, J.N. (2011). Spontaneous firing and evoked pauses in the tonically active cholinergic interneurons of the striatum. Neuroscience *198*, 27–43.

Jin, X., and Costa, R.M. (2010). Start/stop signals emerge in nigrostriatal circuits during sequence learning. Nature *466*, 457–462.

Jones, I.W., Bolam, J.P., and Wonnacott, S. (2001). Presynaptic localisation of the nicotinic acetylcholine receptor beta2 subunit immunoreactivity in rat nigrostriatal dopaminergic neurones. J. Comp. Neurol. *439*, 235–247.

Lambe, E.K., Picciotto, M.R., and Aghajanian, G.K. (2003). Nicotine induces glutamate release from thalamocortical terminals in prefrontal cortex. Neuropsychopharmacology *28*, 216–225.

Léna, C., Changeux, J.P., and Mulle, C. (1993). Evidence for "preterminal" nicotinic receptors on GABAergic axons in the rat interpeduncular nucleus. J. Neurosci. *13*, 2680–2688.

Matsumoto, N., Minamimoto, T., Graybiel, A.M., and Kimura, M. (2001). Neurons in the thalamic CM-Pf complex supply striatal neurons with information about behaviorally significant sensory events. J. Neurophysiol. *85*, 960–976.

Montague, P.R., McClure, S.M., Baldwin, P.R., Phillips, P.E., Budygin, E.A., Stuber, G.D., Kilpatrick, M.R., and Wightman, R.M. (2004). Dynamic gain control of dopamine delivery in freely moving animals. J. Neurosci. *24*, 1754–1759.

Morris, G., Arkadir, D., Nevet, A., Vaadia, E., and Bergman, H. (2004). Coincident but distinct messages of midbrain dopamine and striatal tonically active neurons. Neuron *43*, 133–143.

Owesson-White, C.A., Cheer, J.F., Beyene, M., Carelli, R.M., and Wightman, R.M. (2008). Dynamic changes in accumbens dopamine correlate with learning during intracranial self-stimulation. Proc. Natl. Acad. Sci. USA *105*, 11957–11962.

Phillips, P.E., Stuber, G.D., Heien, M.L., Wightman, R.M., and Carelli, R.M. (2003). Subsecond dopamine release promotes cocaine seeking. Nature *422*, 614–618.

Raz, A., Feingold, A., Zelanskaya, V., Vaadia, E., and Bergman, H. (1996). Neuronal synchronization of tonically active neurons in the striatum of normal and parkinsonian primates. J. Neurophysiol. *76*, 2083–2088.

Redgrave, P., Gurney, K., and Reynolds, J. (2008). What is reinforced by phasic dopamine signals? Brain Res. Brain Res. Rev. *58*, 322–339.

Rice, M.E., and Cragg, S.J. (2004). Nicotine amplifies reward-related dopamine signals in striatum. Nat. Neurosci. *7*, 583–584.

Schultz, W. (2010). Dopamine signals for reward value and risk: basic and recent data. Behav. Brain Funct. *6*, 24.

Smith, Y., Raju, D.V., Pare, J.F., and Sidibe, M. (2004). The thalamostriatal system: a highly specific network of the basal ganglia circuitry. Trends Neurosci. *27*, 520–527.

Surmeier, D.J., Plotkin, J., and Shen, W. (2009). Dopamine and synaptic plasticity in dorsal striatal circuits controlling action selection. Curr. Opin. Neurobiol. *19*, 621–628.

Threlfell, S., and Cragg, S.J. (2011). Dopamine signaling in dorsal versus ventral striatum: the dynamic role of cholinergic interneurons. Front Syst. Neurosci. *5*, 11.

Threlfell, S., Clements, M.A., Khodai, T., Pienaar, I.S., Exley, R., Wess, J., and Cragg, S.J. (2010). Striatal muscarinic receptors promote activity dependence of dopamine transmission via distinct receptor subtypes on cholinergic interneurons in ventral versus dorsal striatum. J. Neurosci. *30*, 3398–3408.

Tsai, H.C., Zhang, F., Adamantidis, A., Stuber, G.D., Bonci, A., de Lecea, L., and Deisseroth, K. (2009). Phasic firing in dopaminergic neurons is sufficient for behavioral conditioning. Science *324*, 1080–1084.

Witten, I.B., Lin, S.C., Brodsky, M., Prakash, R., Diester, I., Anikeeva, P., Gradinaru, V., Ramakrishnan, C., and Deisseroth, K. (2010). Cholinergic interneurons control local circuit activity and cocaine conditioning. Science *330*, 1677–1681.

Wonnacott, S. (1997). Presynaptic nicotinic ACh receptors. Trends Neurosci. *20*, 92–98.

Zhang, H., and Sulzer, D. (2004). Frequency-dependent modulation of dopamine release by nicotine. Nat. Neurosci. *7*, 581–582.